



ELSEVIER

Available online at [www.sciencedirect.com](http://www.sciencedirect.com)

Public Health

journal homepage: [www.elsevier.com/puhe](http://www.elsevier.com/puhe)

## Original Research

# A model for the coupling of the Greater Bairam and local environmental factors in promoting Rift-Valley Fever epizootics in Egypt

H. Gil <sup>a</sup>, W.A. Qualls <sup>a,\*</sup>, C. Cosner <sup>b</sup>, D.L. DeAngelis <sup>c</sup>, A. Hassan <sup>d</sup>,  
A.M. Gad <sup>e</sup>, S. Ruan <sup>b</sup>, S.R. Cantrell <sup>b</sup>, J.C. Beier <sup>a</sup>

<sup>a</sup> Department of Public Health Sciences, University of Miami Miller School of Medicine, Miami, FL, USA

<sup>b</sup> Department of Mathematics, University of Miami, Miami, FL, USA

<sup>c</sup> Department of Biology, University of Miami, Miami, FL, USA

<sup>d</sup> Institute of Environmental Studies and Research, Ain Shams University, Egypt

<sup>e</sup> Department of Entomology, Ain Shams University, Egypt

## ARTICLE INFO

## Article history:

Received 26 June 2014

Received in revised form

13 April 2015

Accepted 9 July 2015

Available online xxx

## Keywords:

Rift-Valley Fever

Epizootics

Global health

Greater Bairam

Modeling

## ABSTRACT

**Objectives:** Rift-Valley Fever (RVF) is a zoonotic mosquito-borne disease in Africa and the Arabian Peninsula. Drivers for this disease vary by region and are not well understood for North African countries such as Egypt. A deeper understanding of RVF risk factors would inform disease management policies.

**Study design:** The present study employs mathematical and computational modeling techniques to ascertain the extent to which the severity of RVF epizootics in Egypt differs depending on the interaction between imported ruminant and environmentally-constrained mosquito populations.

**Methods:** An ordinary differential system of equations, a numerical model, and an individual-based model (IBM) were constructed to represent RVF disease dynamics between localized mosquitoes and ruminants being imported into Egypt for the Greater Bairam. Four cases, corresponding to the Greater Bairam's occurrence during distinct quarters of the solar year, were set up in both models to assess whether the different season-associated mosquito populations present during the Greater Bairam resulted in RVF epizootics of variable magnitudes.

**Results:** The numerical model and the IBM produced nearly identical results: ruminant and mosquito population plots for both models were similar in shape and magnitude for all four cases. In both models, all four cases differed in the severity of their corresponding simulated RVF epizootics. The four cases, ranked by the severity of the simulated RVF epizootics in descending order, correspond with the occurrence of the Greater Bairam on the following months: July, October, April, and January. The numerical model was assessed for sensitivity with respect to parameter values and exhibited a high degree of robustness.

\* Corresponding author. 1120 NW 14th Street, Clinical Research Building, Office 1077A, Miami, FL, 33136, USA. Tel.: +1 904 377 3268.

E-mail addresses: [hgil@med.miami.edu](mailto:hgil@med.miami.edu) (H. Gil), [w.qualls@med.miami.edu](mailto:w.qualls@med.miami.edu) (W.A. Qualls), [gcc@math.miami.edu](mailto:gcc@math.miami.edu) (C. Cosner), [ddeangelis@bio.miami.edu](mailto:ddeangelis@bio.miami.edu) (D.L. DeAngelis), [ali.9973@gmail.com](mailto:ali.9973@gmail.com) (A. Hassan), [adelgad2002@yahoo.com](mailto:adelgad2002@yahoo.com) (A.M. Gad), [ruan@math.miami.edu](mailto:ruan@math.miami.edu) (S. Ruan), [rsc@math.miami.edu](mailto:rsc@math.miami.edu) (S.R. Cantrell), [jbeier@med.miami.edu](mailto:jbeier@med.miami.edu) (J.C. Beier).

<http://dx.doi.org/10.1016/j.puhe.2015.07.034>

0033-3506/© 2015 The Royal Society for Public Health. Published by Elsevier Ltd. All rights reserved.

**Conclusions:** Limiting the importation of infected ruminants beginning one month prior to the Greater Bairam festival (on years in which the festival falls between the months of July and October: 2014–2022) might be a feasible way of mitigating future RVF epizootics in Egypt.

© 2015 The Royal Society for Public Health. Published by Elsevier Ltd. All rights reserved.

## Introduction

Rift-Valley Fever (RVF) is a zoonotic vector-borne disease caused by the Rift-Valley Fever Virus (RVFV).<sup>1</sup> RVF outbreaks have occurred in most of Africa and the Arabian Peninsula since the first reported outbreak of the disease in the Rift-Valley of Kenya in 1931.<sup>2</sup> The emergence of this disease has been steady, expanding out of Sub-Saharan Africa and into Egypt in 1977, Mauritania in 1987, and Saudi Arabia and Yemen in 2000.<sup>3–6</sup> The disease represents a significant burden of morbidity and mortality in these regions, affecting domestic livestock animals (ruminants), and to a lesser extent, humans.<sup>2</sup> The 1977 RVF outbreak in Egypt resulted in an estimated 18,000 infections and 598 deaths in humans.<sup>6</sup> The disease causes death and abortion in young and fetal livestock and minor to fatally severe symptoms in humans.<sup>2</sup> Several risk factors for RVF outbreaks have been identified; among them are strong climate hydrology (heavy rains), high vegetation index, the migration of infected animals, anthropomorphic changes to the environment (dam or irrigation canal construction), and the application of contaminated vaccines to ruminants.<sup>7–11</sup> The relevance of these risk factors varies with respect to geography. In Egypt, the primary RVF vector is the *Culex* mosquito; RVF is transmitted through the bites of RVFV-infected *Culex* mosquitoes to ruminants and from infected ruminants to humans through direct contact with bodily fluids.<sup>12,13</sup> Egypt has had a number of outbreaks occur within its borders since 1977 and many risk factors have been attributed as causes (importation of infected livestock, heavy rains, application of contaminated vaccines).<sup>14–16</sup> However, in many of these cases, the exact causes of these epizootics have not been resolved. A deeper understanding of RVF risk factors in Egypt would inform disease management policies for the prevention and control of RVF outbreaks.

Mathematical modeling has been a prominent tool in the study of infectious disease outbreak drivers. Many risk factors and conditions that potentially contribute to the growth, or mitigation, of RVF in a population have been modeled in numerous studies.<sup>17</sup> However, only a limited number of these studies have focused on how the unique socio-environmental conditions engendered by the Greater Bairam festival influences the risk of an RVF epizootic unfolding.<sup>18,19</sup>

The Greater Bairam is a Muslim holiday, taking place every lunar year, on which participants congregate to pray, and subsequently, sacrifice a livestock animal.<sup>20</sup> In Egypt, tens of thousands of ruminants are imported every year to meet the demand for the festival.<sup>21</sup> Previous studies have suggested

that high livestock densities resulting from importation for the festival, in confluence with high mosquito densities which are present during rainy seasons, creates favorable conditions for RVF epizootics.<sup>22</sup> The present work is a study of this scenario, which as a result of an 11-day disparity between the lunar and solar year lengths, naturally occurs for a contiguous series of years approximately every three decades.

This study mathematically and computationally models a system representing ruminants (some infected with RVFV) being imported into Egypt during the Greater Bairam, while exposed to varying *Culex* mosquito densities during the migration. A novelty of this study, with regards to RVF modeling, is the treatment of numerous risk factors (such as festival-induced livestock importation rate and mosquito-density carrying capacity) as time-dependent parameters, allowing the periodicities of these real phenomena to be mirrored. The study reports measurable differences in simulated RVF epizootic risk given massive livestock importation during different quarters of the solar year.

## Methods

### Model descriptions

A mathematical system of ordinary differential equations consisting of a single patch, representing RVF disease dynamics in Egypt, was constructed (Fig. 1 and 2). Two computational models were then developed: a numerical model and an individual-based model (IBM). The models include ruminant and mosquito populations with the former capable of

$$\begin{aligned}\frac{dS}{dt} &= r_{sus} - \alpha SV - \mu S + \zeta R - \kappa S, \\ \frac{dI}{dt} &= r_{inf} + \alpha SV - (\mu + \gamma + \delta)I - \kappa I, \\ \frac{dR}{dt} &= \gamma I - (\mu + \zeta)R - \kappa R, \\ \frac{dU}{dt} &= \xi(U + V) - \frac{\xi - \nu}{M}(U + V)^2 - \nu U - \beta IU, \\ \frac{dV}{dt} &= -\nu V + \beta IU.\end{aligned}$$

**Fig. 1 – Mathematical Model.** The model is a one-patch system of ordinary differential equations representing RVF disease dynamics in Egypt. Two populations, ruminants and mosquitoes, comprise the system, ruminants serving as carriers of RVFV and mosquitoes serving as vectors.

attaining one of three states (susceptible, infected, and recovered), and the latter able to attain one of two states (uninfected and infected).

The models mimic the importation of ruminants (a fraction of which are infected with RVFV) into Egypt for the Greater Bairam. Upon entering the system (Egypt), ruminants are exposed to the bites of *Culex* mosquitoes. Ruminants have an associated natural mortality that increases if infected with RVFV. Infected ruminants can recover from infection and become immune for a short period of time. The rate of ruminant importation is initially low and begins to increase rapidly two months prior to the festival's occurrence. When the festival arrives, the importation rate decreases dramatically and a slaughter rate takes greater effect. Mosquitoes have associated reproduction and death rates. Mosquito offspring cannot be infected initially (in line with observed RVF mosquito biology in *Culex*).<sup>23</sup> The reproductive rate of mosquitoes is constrained by a sinusoidal carrying capacity synched to a solar period, representing Egypt's climate hydrology.

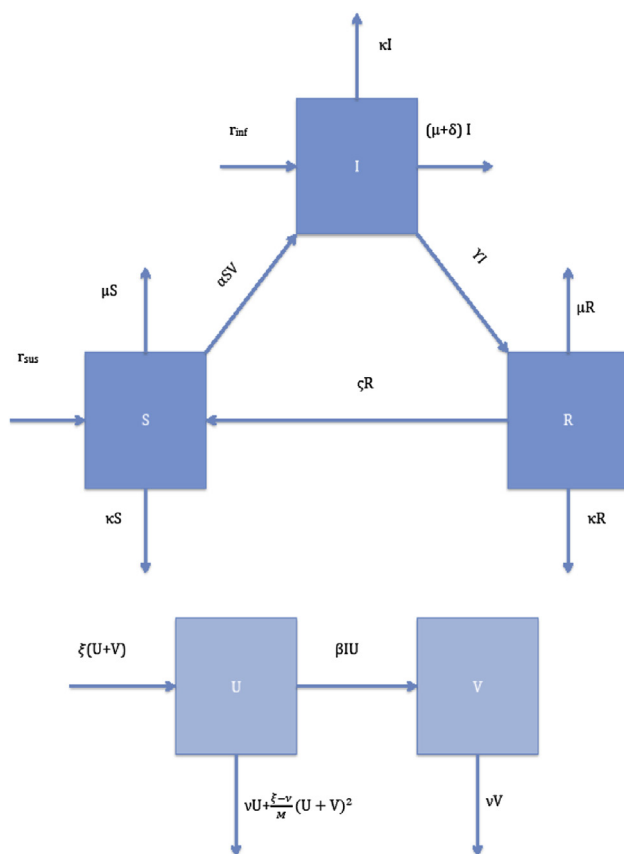


**Fig. 2 – Compartment diagram of the mathematical model.** In the diagram, each compartment (box) represents one of a total of five states attainable by either a ruminant (susceptible, infected, recovered) or a mosquito (uninfected, infected). Arrows pointing from one compartment to another indicate an allowable transition from one state to another. Arrows not pointing to or from a compartment indicate exit of or entry into the system, respectively.

### Model details

The computational models differ in that the numerical model is continuous and deterministic while the IBM is discrete and stochastic. Further differences between the two models include: 1) The IBM simulation being performed on daily time steps, 2) In the IBM, all the parameter values represent rate coefficients, 3) In the IBM, the parameters for all the processes, except the importation rates of the ruminants and mosquitoes, are treated as probabilities. That is, at each time step, a random number is chosen between 0 and 1. If the value is below the value of the rate of change, then the process associated with the parameter occurs.

The models were run to simulate 365 days. Parameter descriptions and values for these models are shown in Tables 1–3. The same parameter values were used for both the numerical model and IBM.

### Seasonal scenarios

In order to investigate whether the timing of massive ruminant importation (with respect to the solar year) affects the severity of a potential RVF epizootic, four cases were studied with each model. Each case corresponds to the Greater Bairam occurring during a different quarter of the solar year:

- Out-of-phase case: The festival occurs in January when mosquito densities are at their lowest point;
- Rise-phase case: The festival occurs in April when mosquito densities are at the midpoint between their lowest and highest points and increasing;
- In-phase case: The festival occurs in July when mosquito densities are at their highest point; and
- Fall-phase case: The festival occurs in October when mosquito densities are at the midpoint between their highest and lowest points and decreasing.

The start of the Greater Bairam occurs on day 91 in both models for all four cases. The different phases of the mosquito density oscillation cycle present when the festival occurs was achieved by transversal shifting of the carrying capacity function by oscillatory period quarters. The mosquito carrying capacities for these four cases are graphically depicted in Fig. 3a.

### Sensitivity analysis

Since standard sophisticated sensitivity analyses were not possible for the numerical model due to the numerous time-dependent parameter functions, rudimentary sensitivity

**Table 1 – State variables of the mathematical model.**

State variable	Description
S	Number of susceptible ruminants at time t
I	Number of infectious ruminants at time t
R	Number of recovered ruminants at time t
U	Number of susceptible mosquitoes at time t
V	Number of infectious mosquitoes at time t

**Table 2 – Physical interpretation of the parameters of the mathematical model.**

Parameter	Description
$I_{sus}$	Importation rate of susceptible ruminants
$I_{inf}$	Importation rate of infectious ruminants
$\mu$	Natural death rate of ruminants
$\delta$	Disease-induced death rate of ruminants
$\kappa$	Slaughter rate of ruminants
$\gamma$	Recovery rate of ruminants
$\zeta$	Rate of loss of immunity of ruminants
$\xi$	Growth rate of mosquitoes
$\nu$	Natural death rate of mosquitoes
$M$	Carrying-capacity of mosquitoes
$\alpha$	Transmission rate from vector to host
$\beta$	Transmission rate from host to vector

analyses were performed instead. In these analyses, the values of individual model parameters for the in-phase case were increased by 10% of the baseline (original parameter values in Tables 2 and 3) and the corresponding changes in cumulative infected ruminant-days (area under the infected ruminant plot) output by the model (referred to as *cumulative infected ruminant-day sum*) were tabulated (Table 4). The percent change in the cumulative infected ruminant-day sum (referred to as CIRDS-PC) for each parameter value was then calculated as follows:

CIRDS-PC (parameter) = (10% parameter increase – baseline)/baseline.

A positive CIRDS-PC value indicated a net positive change in the cumulative number of infected ruminant-days resulting

from a positive percent increase in the value of a specific parameter; negative CIRDS-PC values indicated a net negative change in the number of infected ruminant-days resulting from the parameter value increase. Note that the magnitudes of the CIRDS-PC are also informative for comparing the sensitivity of different model parameters.

In the context of these model simulations, CIRDS-PC values serve as a standard measure by which to compare the effects of changing different parameter values, and aid in testing model robustness. As a practical measure in evaluating disease control strategies, CIRDS-PC values assist in assessing the relative effects of targeting potential risk factors (variables/parameters) in these models and whether such efforts are expected to result in mitigation or exacerbation of RVF epizootics.

## Results

The quantities of infected ruminants produced by the numerical model and the IBM during the course of the simulations are plotted in Fig. 4a and b. These figures show that infected ruminant levels increase consistently in both models until they reach a maximum on day 91, after which infected ruminant levels drop and approach zero. A small hump can be observed around day 100 in both models. This small hump represents a rebound in ruminant quantities after the temporarily enhanced ruminant slaughter rate is minimized one week after the start of the Greater Bairam (day 98), due to the conclusion of the festival. The small hump is an artifact of

**Table 3 – Parameter values of the models.**

Parameter	Value	Units	Reference
$I_{sus}$	$\begin{cases} 1500e^{-(t-91)^2/625} & 0 \leq t < 91 \\ 1500e^{-(t-91)^2/25} & 91 \leq t \leq 365 \end{cases}$	1/day	21 a
$I_{inf}$	$\begin{cases} 500e^{-(t-91)^2/625} & 0 \leq t < 91 \\ 500e^{-(t-91)^2/25} & 91 \leq t \leq 365 \end{cases}$	1/day	26 b
$\mu$	1/3650	1/day	27
$\delta$	0.0312	1/day	27
$\kappa$	$\begin{cases} 0.9 & 91 \leq t \leq 98 \\ 0.1 & t < 91 \text{ or } t > 98 \end{cases}$	1/day	–
$\gamma$	0.14	1/day	27
$\zeta$	8/365	1/day	28
$\xi$	1/12	1/day	–
$\nu$	1/40	1/day	27
$M$	$40000 \sin\left(\frac{2\pi}{365}t - \phi\right) + 50000$ $\phi = \begin{cases} 0 & \text{In} \\ \pi/2 & \text{Rise} \\ \pi & \text{Out} \\ 3\pi/2 & \text{Fall} \end{cases}$	–	–
$\alpha$	0.00001	1/day	29
$\beta$	0.000001	1/day	29

<sup>a</sup> This reference in Table 3 provided an estimate for the total number of ruminants imported into Egypt for the Greater Bairam which the respective parameter function approximates in order of magnitude.

<sup>b</sup> This reference in Table 3 provided an estimate for the proportion of infected ruminants in Sudan which the respective parameter function approximates.

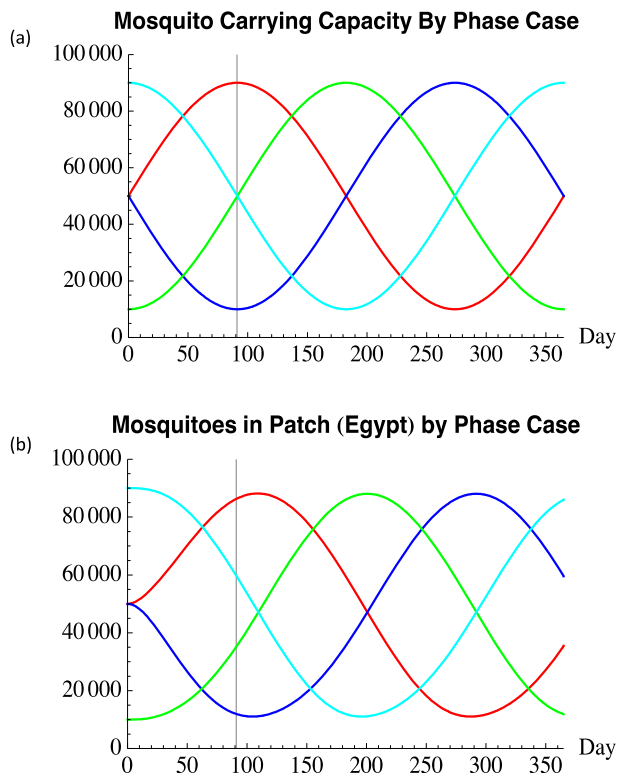


**Fig. 3 – (a) Mosquito Carrying Capacity By Case. In this diagram, time-dependent mosquito carrying capacities are plotted for each of the four phase cases: In-phase (red), Out-of phase (blue), Rise-phase (green), Fall-phase (cyan). The black vertical line at day 91 marks the time at which the Greater Bairam begins for all cases and for both the IBM and the numerical model. (b) Mosquitoes Produced by Numerical Model. The number of mosquitoes (both uninfected and infected) produced by the numerical model closely follows the mosquito carrying capacity, albeit with a two week lag which mimics real *Culex* mosquito biology. The same behavior is present in the IBM (not shown). (For interpretation of the references to colour in this figure legend, the reader is referred to the web version of this article.)**

**Table 4 – Sensitivity analysis: Percent change in cumulative infected ruminant-day sum for each parameter.**

Parameter	CIRDS-PC
$r_{sus}$	+3.87
$r_{inf}$	+9.55
$\mu$	-0.02
$\delta$	-1.49
$\kappa$	-3.74
$\gamma$	-6.25
$\zeta$	+0.13
$\xi$	+0.49
$\nu$	-0.94
$M$	+3.36
$\alpha$	+3.45
$\beta$	+3.39

the system equilibrating after the slaughter rate's value was instantaneously decreased.

Close-ups of the same model outputs (Fig. 4c and d) reveal additional similarities between the two models. For instance, the infected ruminant plot for each of the four cases is similarly shaped, and in close agreement in terms of magnitudes, between the two models. In both models, all four cases differed in the severity of their corresponding simulated RVF epizootics. The in-phase case was the case that produced the greatest number of infected ruminants during festival time, followed by the fall-phase case, the rise-phase case, and lastly the out-of-phase case. Thus, the four cases, ranked by the severity of the simulated RVF epizootics in descending order, correspond with the occurrence of the Greater Bairam on the following months: July, October, April, and January. This implies that, during this time frame, the former cases had a larger vector population available to amplify the virus in the ruminant population, particularly in the month before the festival occurs (when ruminant importation rates rapidly increase).

Given that the numerical model is deterministic, all of the information needed to interpret the results for this model is available in Fig. 4a and c. The IBM, however, is stochastic and thus requires a measure of variation in order to properly interpret its results with some certainty. Fig. 5 addresses this aspect by complementing Fig. 4b and d in demonstrating that the mean of infected ruminants around the time of the Greater Bairam for a particular phase case lies several standard deviations apart from that of any other phase case (means and standard deviations were averaged or measured over 10 runs). In all, these results demonstrate a statistically significant difference in the severity of the simulated RVF epizootics in the IBM for all four cases, and support the previously mentioned severity rank for the cases.

## Discussion

The results of this study are in line with the research literature. That concurrently high ruminant and mosquito densities can increase the likelihood of an RVF epizootic is a long-standing hypothesis in the literature. Abdo-Salem et al. found empirical support for this hypothesis when identifying the year 2000 as distinct among other years in Yemen, in that the Greater Bairam (and associated ruminant importation) occurred concomitant with strong rainy seasons (which promote mosquito growth); this unique scenario could explain the development of an RVF outbreak that year.<sup>18</sup> Our study found empirical support for this hypothesis as well, but in addition, we found that massive ruminant importation that occurs three months after mosquito densities have peaked (and are still subsiding) leads to an equivalently severe situation in terms of potential RVF-infected ruminant quantities. Thus, an additional scenario is as significant and requires the same level of attention and risk mitigation than was previously anticipated.

Among the strengths of this work is the implementation of both a numerical model and an IBM, allowing for patterns, arising from the output of each model, to be compared, and for

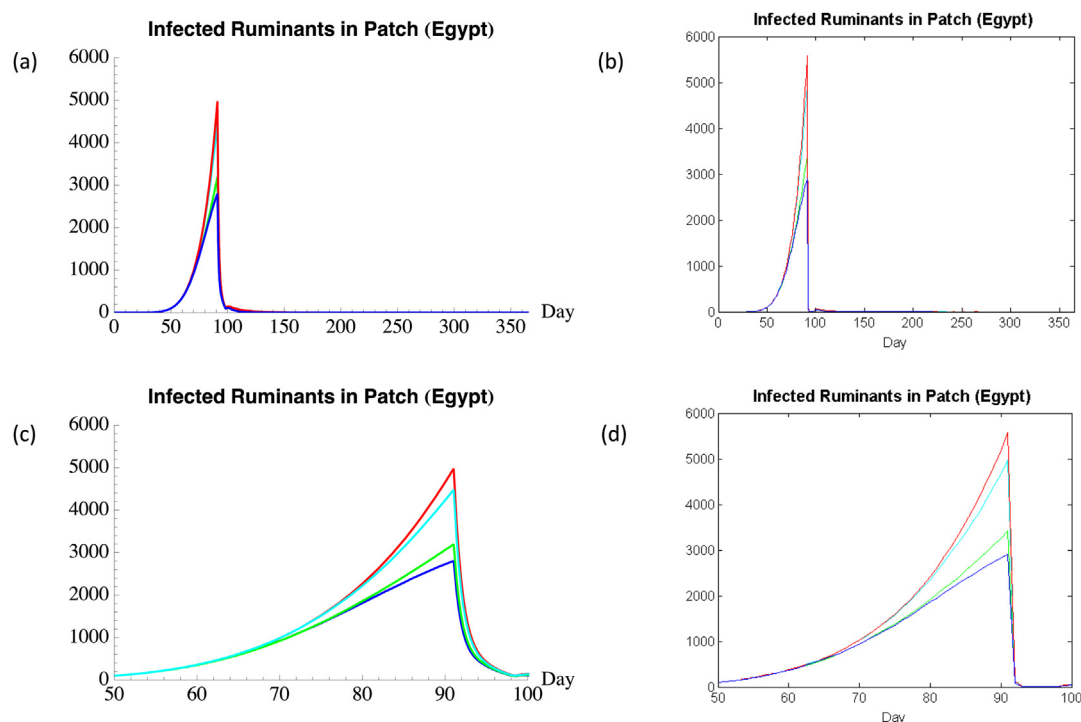


**Fig. 4 – (a) Infected Ruminants Produced By Numerical Model; (b) Infected Ruminants Produced By Individual-Based Model; (c) Infected Ruminants Produced By Numerical Model (Close-Up); (d) Infected Ruminants Produced By Individual-Based Model (Close-Up).** In descending order, the phase case for which the number of infected ruminants is greatest during festival time is: in-phase (red), fall-phase (cyan), rise-phase (green), out-of-phase (blue). Results for both models are similar. The number of infected ruminants at any time in the IBM is within 10% of the number of infected ruminants in the numerical model at that time. (For interpretation of the references to colour in this figure legend, the reader is referred to the web version of this article.)

similar patterns to be attributable to the system dynamics rather than to the idiosyncrasies of distinct computational methods. Another feature is the utilization of time-dependent parameters with periodic behavior that closely mimics that of real phenomena (i.e., climate hydrology and ruminant importation patterns).

The main limitations of this study stemmed from a lack of available information regarding the appropriate magnitude for the *Culex* mosquito's carrying capacity. This in turn led to significant uncertainty for a few of our model parameter values. However, our careful calibration of model parameters with the values that were available in the literature produced realistic ruminant and mosquito population trends. Particularly, the population of mosquitoes (uninfected and infected) produced by the numerical model (Fig. 3b) and the IBM is consistent with mosquito *Culex* mosquito biology in that the mosquito population closely follows the carrying capacity, albeit with a two week lag which is evident in Fig. 3b.

The use of time-dependent model parameters precluded us from employing standard methods for evaluating the sensitivity of model parameters. However, our extensive experimentation with modifying these parameter values did not result in large changes in the models' outputs: population plots maintained the same shape, the same trends described earlier, and approximately the same magnitude. The CIRDS-PC values in Table 4 suggest that limiting the importation of

infected ruminants is one (if not the most) effective way by which to reduce the risk of an RVF epizootic emerging.

We understand that using a single patch to represent the entire region of Egypt is a strong idealization given that the true disease system would require several geographic regions (i.e., patches) to be taken into account in order to be realistically modeled. This assumption was made to facilitate insight into the behavior of the disease system. A realistic model would be too complex to be amenable to such understanding. Our single patch model serves as a starting point for more realistic and spatially-detailed models.

We believe that capturing the variability of important dynamical processes and incorporating such behavior into models could reveal RVF risk patterns that would otherwise be overlooked. Moving forward, we plan to build a theoretical framework to calculate  $R_0$  values for systems that incorporate time-dependent parameters, as well as expand the system described in the present study to include multiple patches, and incorporate time delays in the migration of ruminants between patches.

Drivers for RVF have been studied extensively since the 1970s. Scientific understanding of RVF risk factors along the Eastern and Southern coast of Africa has progressed to the point where epizootics in these regions can be predicted considerably in advance.<sup>24,25</sup> However, a firm understanding of RVF dynamics in the Northern Africa region has been

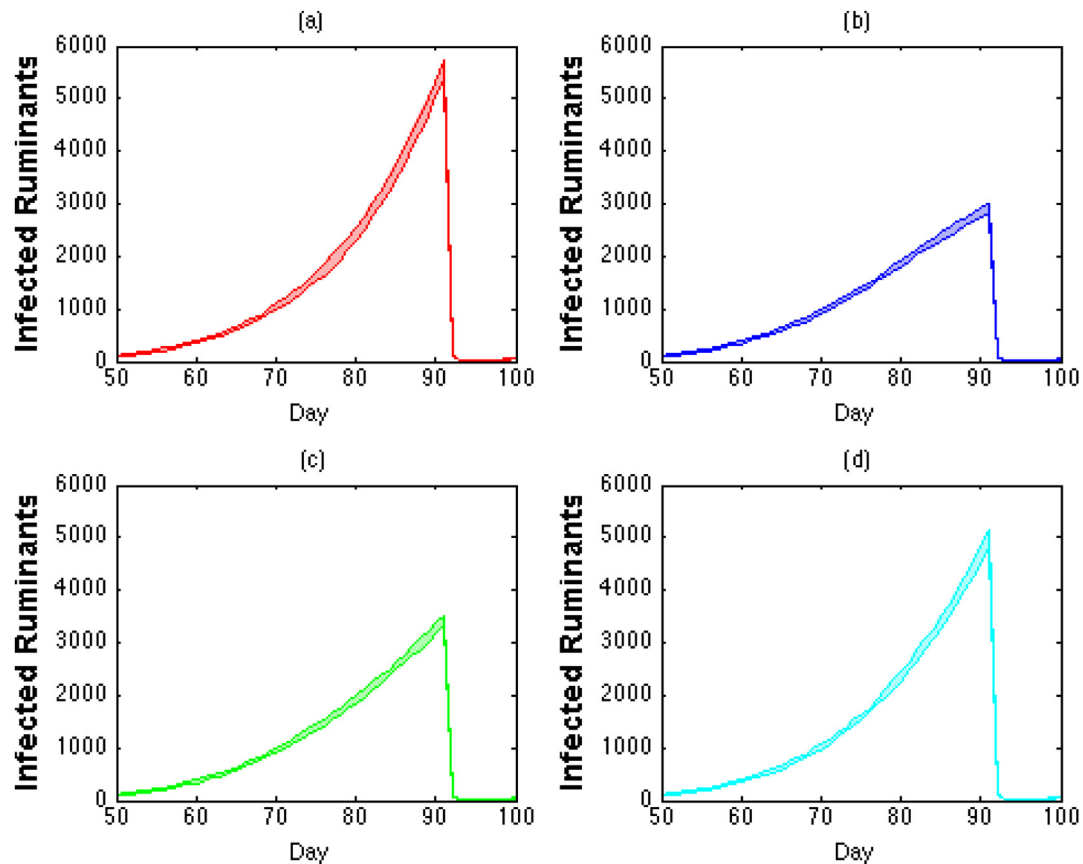


**Fig. 5 – Infected Ruminants Produced By Individual-Based Model (With Interval).** The average number of infected ruminants (with interval of  $\pm 2$  standard deviations) generated by the IBM over the course of a simulated year for all four phase cases: (a) in-phase (red); (b) out-of-phase (blue); (c) rise-phase (green); (d) fall-phase (cyan). (For interpretation of the references to colour in this figure legend, the reader is referred to the web version of this article.)

elusive. Such has been the case in Egypt where RVF epizootics are considered to occur sporadically because causal factors have not been identified despite five confirmed epizootics having occurred since 1977. The identification of causal factors in Egypt has been complicated by numerous inextricable factors that create insurmountable uncertainty as to the mechanism(s) of RVF epizootic development. Yet, understanding RVF risk factors is of fundamental importance to the design and implementation of disease management policies for preventing and controlling RVF.

This study models a controlled system, in which large quantities of ruminants are imported periodically and exposed to oscillatory mosquito populations, and demonstrates that in such a system, the expected severity of a potential RVF epizootic changes every year and follows a regular pattern. All other things equal, the severity of a potential RVF epizootic is optimal when high densities of ruminants are present during, and soon after, the presence of high mosquito densities. In Egypt, such a situation occurs when the Greater Bairam takes place between the months of July and October. Due to limited historical data, this mechanism for RVF outbreak development is difficult to rigorously confirm.

Our work suggests that limiting the importation of infected ruminants beginning one month prior to the Greater Bairam

festival (on years in which the festival falls between the months of July and October: 2014–2022) might be a feasible way of mitigating future RVF epizootics in Egypt. These findings can be communicated to the Egyptian Ministry of Agriculture (MoA) to support the implementation of risk mitigation efforts. RVF epizootics are an issue that the Egyptian MoA is highly cognizant of and has taken measures to prevent; in 2013, the MoA imported ruminants from disease-free countries.<sup>21</sup> Additional steps that can be taken include the strengthening and enforcement of medical examination at the Egyptian border to identify and obstruct the illegal importation of RVFV-infected ruminants.

## Author statements

## Acknowledgements

We want to thank Karina Lizzi for her guidance and comments on the manuscript. All data collected was open access and provided by the co-authors.

## Ethical approval

Ethical approval was not needed for the current study.

### Funding

Research was supported by the National Institute of Health (NIH) grant R01GM093345.

### Competing interests

The authors declare that they have no competing interests.

### Authors' contributions

HG: developed the analytical model, finalized the IBM, analyzed both models, and wrote the manuscript.

WAQ: provided guidance and insight regarding mosquito behavior and biology.

JB: provided guidance and insight regarding mosquito ecology in Egypt and Sudan.

CC: provided assistance with the design of the analytical model and interpretation of the results.

DD: developed the first version of the IBM and helped to finalize its integrity.

AH: provided Nile River data from the Egyptian Ministry of Agriculture, mosquito density data from personal studies, insight into the mosquito ecology of Egypt, and insight into importation trends in Egypt during the Greater Bairam.

SR: provided guidance and insight regarding mathematical modeling of mosquito ecology.

SC: provided guidance and insight regarding mathematical modeling of mosquito ecology.

### REFERENCES

1. Daubney RJ, Hudson JR, Garnham PC. Enzootic hepatitis of Rift Valley fever: an undescribed virus disease of sheep, cattle and man from East Africa. *J Pathol Bacteriol* 1931;34:543–79.
2. The Centers for Disease Control and Prevention: Rift Valley Fever Fact Sheet [%3ca href=http://www.cdc.gov/ncidod/dvrd/spb/mnpages/dispages/Fact\_Sheets/Rift\_Valley\_Fever\_Fact\_Sheet.pdf].
3. Meegan JM. The Rift Valley fever epizootic in Egypt 1977–1978. 1. Description of the epizootic and virological studies. *Trans R Soc Trop Med Hyg* 1979;73:618–23.
4. Hoogstraal H, Meegan JM, Khalil GM. The Rift Valley fever epizootic in Egypt 1977–1978. 2. Ecological and entomological studies. *Trans R Soc Trop Med Hyg* 1979;73:624–9.
5. Jouan A, Le Guenno B, Digoutte JP, Philippe B, Riou O, Adam F. An RVF epidemic in southern Mauritania. *Ann Inst Pasteur Virol* 1988;139:307–8.
6. Madani TA, Al-Mazrou YY, Al-Jeffri MH, Mishkhas AA, Al-Rabeah AM, et al. Rift Valley fever epidemic in Saudi Arabia: epidemiological, clinical, and laboratory characteristics. *Clin Infect Dis* 2003;37:1084–92.
7. Davies FG, Linthicum KJ, James AD. Rainfall and epizootic Rift Valley fever. *Bull World Health Organ* 1985;63:941–3.
8. Anyamba A, Linthicum KJ, Mahoney R, Tucker CJ, Kelley PW. Mapping potential risk of Rift Valley fever outbreaks in african savannas using vegetation index time series data. *Photogrammetric Eng Remote Sens* 2002;68:137–45.
9. Gad AM, Feinsod FM, Allam IH, Eisa M, Hassan AN, Soliman BA, et al. A possible route for the introduction of Rift Valley fever virus into Egypt during 1977. *J Trop Med Hyg* 1986;89:233–6.
10. Gerdes GH. Rift Valley fever. *Rev Sci Tech Off Int Epiz* 2004;23:613–23.
11. Kamal S. Observations on Rift Valley fever virus and vaccines in Egypt. *Virol J* 2011;8:532–40.
12. Meegan JM, Khalil GM, Hoogstraal H, Adham FK. Experimental transmission and field isolation studies implicating *Culex pipiens* as a vector of Rift Valley fever virus in Egypt. *Am J Trop Med Hyg* 1980;29:1405–10.
13. Hanafi HA, Fryauff DJ, Saad MD, Soliman AK, Mohareb EW, Medhat I, et al. Virus isolations and high population density implicate *Culex antennatus* (Becker) (Diptera: Culicidae) as a vector of Rift Valley fever virus during an outbreak in the Nile Delta of Egypt. *Acta Trop* 2011;119:119–24.
14. Imam IZE, El Karamany R, Darwish MA. An epidemic of Rift Valley fever in Egypt. *Bull World Health Organ* 1979;57:441–3.
15. Arthur RR, el-Sharkawy MS, Cope SE, Botros BA, Oun S, Morrill JC, et al. Recurrence of Rift Valley fever in Egypt. *Lancet* 1993;342:1149–50.
16. el-Rahim IHA, el-Hakim UA, Hussein M. An epizootic of Rift Valley fever in Egypt in 1997. *Rev Sci Tech Off Int Epiz* 1999;18:741–8.
17. Métras R, Collins LM, White RG, Alonso S, Chevalier V, Thuraniira-McKeever C, et al. Rift Valley fever epidemiology, surveillance, and control: what have models contributed? *Vector Borne Zoonotic Dis* 2011;6:761–71.
18. Abdo-Salem S, Tran A, Grosbois V, Gerbier G, Al-Qadasi M, Saeed K, et al. Can environmental and socioeconomic factors explain the recent emergence of Rift Valley fever in Yemen, 2000–2001? *Vector Borne Zoonotic Dis* 2011;11:773–9.
19. Gao D, Cosner C, Cantrell RS, Beier JC, Ruan S. Modeling the spatial spread of Rift Valley fever in Egypt. *Bull Math Biol* 2013;75:523–42.
20. Aljazeera: millions of muslims around the world observed Eid al-Adha, one of Islam's most poignant religious holidays [%3ca href=http://www.aljazeera.com/indepth/inpictures/2013/10/pictures-eid-al-adha-2013101765553311343.html].
21. The Cairo Post: tens of thousands of livestock imported for Eid al-Adha [%3ca href=http://thecairopost.com/news/8725/news/tens-of-thousands-of-livestock-imported-for-eid-al-adha].
22. Davies FG. Risk of a rift Valley fever epidemic at the haj in Mecca, Saudi Arabia. *Rev Sci Tech Off Int Epiz* 2006;25:137–47.
23. Romoser WS, Oviedo MN, Lerdthusnee K, Patrican LA, Turell MJ, Dohm DJ, et al. Rift Valley fever virus-infected mosquito ova and associated pathology: possible implications for endemic maintenance. *Res Rep Trop Med* 2011;2:121–7.
24. Anyamba A, Chretien JP, Small J, Tucker CJ, Formenty PB, Richardson JH, et al. Prediction of a Rift Valley fever outbreak. *PNAS* 2009;106:955–9.
25. Anyamba A, Linthicum KJ, Small J, Britch SC, Pak E, de La Rocque S, et al. Prediction, assessment of the Rift Valley fever activity in East and Southern Africa 2006–2008 and possible vector control strategies. *Am J Trop Med Hyg* 2010;83:43–51.
26. Eisa M. Preliminary survey of domestic animals of the Sudan for precipitating antibodies to Rift Valley fever virus. *J Hyg (Lond)* 1984;93:629–37.
27. Xue L, Scott HM, Cohnstaedt LW, Scoglio C. A network-based meta-population approach to model Rift Valley fever epidemics. *J Theor Biol* 2012;306:129–44.
28. Pepin M, Bouloy M, Bird BH, Kemp A, Paweska J. Rift Valley fever virus (Bunyaviridae: Phlebovirus): an update on pathogenesis, molecular epidemiology, vectors, diagnostics and prevention. *Vet Res* 2010;41:1–40.
29. Gaff HD, Hartley DM, Leahy NP. An epidemiological model of Rift valley fever. *Electron J Diff Equ*; 2007::1–12.